Quenched-in vacancies in Fe_3Al based alloys: a positron annihilation study

2011 J. Phys.: Conf. Ser. 265 012016

(http://iopscience.iop.org/1742-6596/265/1/012016)

Journal of Physics: Conference Series **265** (2011) 012016 doi:10.1088/1742-6596/265/1/012016

Quenched-in vacancies in Fe_3Al based alloys: a positron annihilation study

O Melikhova[1], J Čížek[1], J Kuriplach[1], I Procházka[1], F Lukáč[1], M Cieslar[1], W Anwand[2] and G Brauer[2]

[1] Charles University in Prague, Faculty of Mathematics and Physics, V Holešovičkách 2, 180 00 Prague 8, Czech Republic
[2] Institut für Strahlenphysik, Forschungszentrum Dresden-Rossendorf, Postfach 510119, D-01314, Dresden, Germany

E-mail: oksivmel@yahoo.com

Abstract. In the present contribution, high-resolution positron lifetime spectroscopy and slow positron implantation spectroscopy are used to characterize defects in $Fe_{75.99}Al_{24.01}$ and $Fe_{71.98}Al_{28.02}$ alloys. In order to facilitate defect identification, we also perform a theoretical study of basic vacancy-like defects in three phases of the Fe_3Al system: ordered ($D0_3$), short-range ordered (B2) and disordered (A2). Positron characteristics, i.e. positron lifetime and positron binding energy to defects are calculated from the first principles for various defect configurations. The results are discussed in the context of experimental data obtained here and available in literature.

1. Introduction

Intermetallic alloys based on the Fe_3Al system represent perspective materials for industrial applications at elevated temperatures due to a number of advantageous features such as a low density, a high strength and a good corrosion resistance. It is also their low cost, which makes these alloys attractive for industry. Very interesting property of Fe_3Al-based alloys is low formation energy of vacancies. The equilibrium concentration of thermal vacancies observed in Fe_3Al-based alloys at high temperatures appears to be as high as several at.% [1]. Several experimental works reported that vacancies have a significant impact on hardness of Fe_3Al based alloys [2-4]. By quenching from elevated temperatures, a high concentration of non-equilibrium vacancies can be retained at room temperature.

Hence it is obvious that a detailed investigation of vacancies in Fe_3Al based alloys is indispensable for a deeper understanding of physical properties of these materials. Positron annihilation spectroscopy (PAS) is a well-recognized, non-destructive method exhibiting very high sensitivity to open-volume defects like vacancies and related defects. [5,6]. The PLS method was applied to defect studies in Fe-Al alloys several times [7-10]. For instance, Schaefer et al. [7,8] performed extensive PLS measurements in situ in a wide temperature interval in order to deduce activation energies of vacancy formation and migration in Fe-Al alloys. A PLS investigation of binary Fe-Al alloys with varying Al content and quenched from 1000°C was carried out by Diego et al. [10].

Although previous papers on Fe-Al based alloys have brought a valuable knowledge, one has to state that most of the earlier PLS measurements on Fe-Al were performed using spectrometers with

relatively poor time resolution (for example 320 ps in [7,8]) and low statistics. Due to these reasons, a reliable decomposition of positron lifetime spectra into individual components could not be performed and only the mean lifetimes (i.e. weighted averages of individual lifetimes) were determined in these works. It was also not possible to include more kinds of defects in the analysis of experimental spectra (e.g. mono- and di-vacancies). Theoretical calculations of positron lifetimes were performed in [10] for several types of defects, for example for different vacancy sites in Al and Fe sublattices as well as for a vacancy-antisite atom defect complex.

The aim of the present work is to characterise the nature of defects in quenched-in Fe_3Al based alloys with over- and under-stoichiometric Al content. Defect studies were performed by two complementary PAS techniques: high resolution positron lifetime (LT) spectroscopy and slow positron implantation spectroscopy (SPIS). The combination of LT and SPIS enables to determine even a very high concentration of vacancies typical for Fe_3Al alloys. PAS investigations were accompanied by Vickers microhardness testing. First principles calculations of positron lifetimes and binding energies to vacancies have been performed in order to characterise different vacancy-type defects that can be present in the studied samples.

2. Computational methods

Positron calculations of basic vacancy-like defects in different phases of the Fe_3Al system [11]: ordered ($D0_3$), short range ordered (B2) and disordered (A2), were performed employing the so-called atomic superposition (ATSUP) method [12]. The lattice parameter used in calculations was a = 5.792 Å [13]. We employed the supercell approach, considering 1024 atom-based supercells. Monovacancies were created by removing one Al or Fe atom. Supercells for B2 and A2 structures were prepared by randomly filling atomic positions in the corresponding sublattice. The electron-positron correlations were treated according to Boroński-Nieminen (BN) [14] and according to the gradient-correction (GC) scheme formulated by Barbiellini et al. [15].

3. Experimental details

In the present work we studied $Fe_{75.99}Al_{24.01}$ and $Fe_{71.98}Al_{28.02}$ alloys, which represent Fe_3Al based alloys with under-stoichiometric and over-stoichiometric Al content. Studied alloys were annealed at 1000^{o}C for 1h in vacuum (10^{-3} mbar) encapsulated in silicon glass ampoules. The annealing treatment was finished by quenching of the silicon glass ampoule into water of room temperature. As the annealing was performed in the disordered A2 phase region, it is expected that A2 is at least partially retained in the quenched samples. However domains transferred into the B2 phase and even a small fraction of the ordered $D0_3$ phase should be expected in the quenched samples despite a high cooling rate.

A $^{22}Na_2CO_3$ positron source with an activity of 1.2 MBq deposited on a 2 μm thick Mylar foil was used for LT studies. The source contribution consists of two weak components with lifetimes $\tau_2 \approx 368$ ps and $\tau_3 \approx$ 1.5 ns. A high resolution digital spectrometer [16,17] was employed for LT investigations of studied alloys. The detector part of the digital LT spectrometer is equipped with two Hamamatsu H3378 photomultipliers coupled with BaF_2 scintillators. Detector pulses are sampled in real time by two ultra-fast 8-bit digitizers Acqiris DC211 with a sampling frequency of 4 GHz. The digitized pulses are acquired in a PC and worked out off-line by a software using a new algorithm for integral constant fraction timing [18]. The time resolution of the digital LT spectrometer was 150 ps (FWHM, ^{22}Na). At least 10^7 annihilation events were accumulated in each LT spectrum.

SPIS studies were performed on the magnetically guided variable energy positron beam "SPONSOR" [19]. The energy of incident positrons was varied in the range from 0.03 to 36 keV. The Doppler broadening of the annihilation line was measured by an HPGe detector with an energy resolution of (1.09 ± 0.01) keV at 511 keV and evaluated in terms of the S parameter.

Microhardness was examined using the Vickers method with a loading of 100 g applied for 10 s (HV0.1) using the STRUERS Duramin-2 micro-tester device.

4. Results and discussion

4.1. Theoretical calculations

Figure 1 shows the unit cell of the $D0_3$ structure. It consists of two interpenetrating simple cubic sublattices denoted A and B. The Fe and Al occupation of the sites in both sublattices differs in three phases existing in the Fe_3Al system:

1. In the case of the complete $D0_3$ order, the A sublattice is occupied exclusively by Fe atoms. The B sublattice consists of alternating sites occupied by Fe and Al atoms. All atoms in the B sublattice are surrounded by 8 nearest neighbor (NN) Fe atoms. Thus, one can distinguish two types of Fe atoms in the $D0_3$ phase: (i) Fe(A) atoms which occupy the A sublattice and are surrounded by 4 NN Fe atoms and 4 NN Al atoms, and (ii) Fe(B) atoms located in the B sublattice surrounded by 8 NN Fe atoms. All Al atoms in the $D0_3$ phase have 8 NN Fe atoms.
2. As for the B2 order in the Fe_3Al system, Fe and Al atoms occupy all sites in the B sublattice with equal probability, while the A sublattice is occupied only by Fe atoms.
3. Finally, in the disordered A2 phase all sites in both sublattices are occupied randomly by Fe or Al atoms.

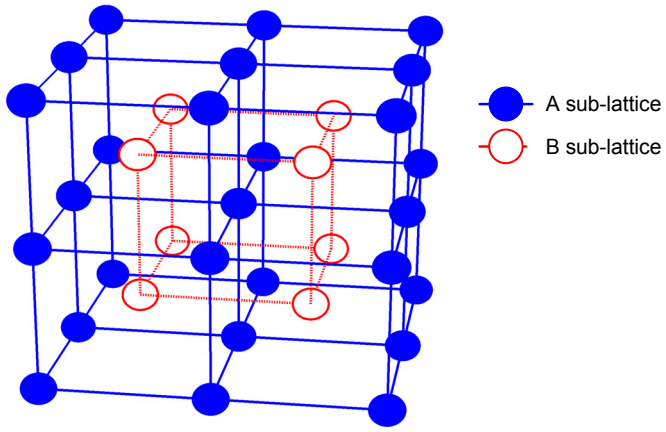

Figure 1. The unit cell of Fe_3Al based alloys showing A and B sublattices.

Positron lifetimes were first calculated using both ATSUP-BN and ATSUP-GC approaches. It is known that the GC scheme is more sensitive to details of the electronic structure than local density approximation (LDA) based approaches [20], like the BN one. Therefore, the GC approach should rather be used with self-consistent electron densities. On the other hand, within the BN approach one can observe a feedback effect, which keeps the positron lifetime unchanged independently of small transfers of the electron density [12] (see also [20]). To this end, positron lifetimes calculated by the ATSUP-BN approach are usually in a better agreement with experiment than lifetimes calculated using the ATSUP-GC approach [20,21]. We can demonstrate this for the case of the bulk lifetime for the $D0_3$ ordered Fe_3Al alloy. The bulk positron lifetime 110 ps calculated using the ATSUP-BN approach is in good agreement with an experimental value of 112 ps [7], while a bulk lifetime of 118 ps calculated with the ATSUP-GC approach is clearly too long. For these reasons, only lifetimes calculated using the ATSUP-BN approach will be considered in this paper. Bulk positron lifetimes and lifetimes of positrons trapped in vacancies calculated using the ATSUP-BN scheme are collected in table 1. Positron binding energies to vacancies (E_b) are shown in table 1 as well. The value of E_b for a given type of vacancy is calculated as a difference of the ground state energy E_0 of the delocalized positron and the energy E_V of the positron trapped in the vacancy considered, i.e.

$$E_b = E_0 - E_V \ . \tag{1}$$

In the $D0_3$ phase one can find three types of vacancies: the Al one and two different Fe ones (in A and B sublattice). Lifetimes of positrons trapped in all types of vacancies fall in the relatively narrow

range from 182 to 187 ps. The longest positron lifetime was found for the Fe vacancy in the A sublattice, i.e. the only vacancy with some NN Al atoms (all the other types of vacancies have only Fe nearest neighbors). Diego et al. [10] suggested that triple defects consisting of two adjacent Fe vacancies in the A sublattice bound to a NN Al atom in the B sublattice are formed in B2 regions at high temperatures. This defect which corresponds to a Fe divacancy in the $D0_3$ phase aligned along the [100] direction was also considered in the calculations, see table 1.

Table 1. Bulk lifetimes, lifetimes of positrons trapped in vacancies, and corresponding positron binding energies *(E_b)* for vacancies calculated using the ATSUP-BN approach for various phases in Fe_3Al. First and second nearest neighbours of examined vacancy configurations are listed in the second and third column, respectively.

annihilation site	vacancy nearest neighbors (NN)	vacancy next nearest neighbors (2NN)	τ (ps)	E_b (eV)
$D0_3$ phase				
Bulk			110	-
Fe vacancy (A sublattice)	4 Al + 4 Fe	6 Fe	187	3.1
Fe vacancy (B sublattice)	8 Fe	6 Al	185	3.2
Al vacancy (B sublattice)	8 Fe	6 Fe	182	3.5
Fe divacancy (A sublattice) in [100] direction	6 Fe + 6 Al	10 Fe	195	4.0
B2 phase				
Bulk			109	-
Fe vacancy (A sublattice)	8 Fe	6 Fe	181	3.1
Fe vacancy (A sublattice)	8 Al	6 Fe	193	2.7
vacancy in B sublattice	8 Fe	6 Fe	182	3.5
vacancy in B sublattice	8 Fe	6 Al	185	3.1
A2 phase				
Bulk			108	-
Vacancy	8 Fe	6 Fe	181	3.1
Vacancy	8 Al	6 Al	199	3.6

The bulk positron lifetime in the partially ordered B2 phase varies due to the random occupation of the B sublattice sites by Fe and Al atoms. To estimate these variations, we calculated bulk positron lifetimes for a set of randomly generated B2 supercells. The mean value of calculated bulk lifetimes from this set is shown in table 1 and is very close to the bulk lifetime obtained for the $D0_3$ phase. The dispersion (standard deviation) of the bulk lifetime in B2 phase was found to be only 0.2 ps. Hence, the effect of the random occupation of the B sublattice sites on the positron lifetime can be considered as negligible.

In the B2 phase one can distinguish Fe vacancies in the A sublattice and vacancies in the B sublattice. The latter vacancies have always 8 NN Fe atoms. On the other hand, number of NN Al and Fe atoms surrounding Fe vacancies in the A sublattice varies randomly. Two extreme cases may be considered for Fe vacancies in the A sublattice in the B2 phase: (i) a vacancy with 8 NN Fe atoms and (ii) a vacancy with 8 NN Al atoms. The local surrounding of Fe vacancies in the A sublattice varies between these two extremes, thereby, the lifetime of trapped positrons is expected to vary between the lifetimes of positrons trapped in Fe vacancy (i) and (ii), i.e. in the range from 181 to 193 ps (see table 1). Figure 2 shows lifetimes of positrons trapped in the Fe vacancy as a function of the number of NN

Al atoms surrounding the vacancy. It is clear that the positron lifetime increases with the increasing number of NN Al atoms. It should be noted that while 2NN of Fe vacancies considered in figure 2 are always Fe atoms (sites on the A sublattice), occupation of third and higher-order NN vary due to the random occupation of the B sublattice sites. Nevertheless, we found that the dispersion of positron lifetimes due to this effect is lower than 0.1 ps for all vacancies considered in figure 2. Thus, the lifetime of trapped positrons is determined predominantly by NN and 2NN atoms surrounding vacancy. Fe vacancies in the A sublattice in the $D0_3$ phase are always surrounded by 4 NN Al atoms. Hence, the Fe-vacancy in the A sublattice surrounded by more than 4 NN Al atoms may be considered also as a vacancy in the $D0_3$ phase with corresponding number of Al antisite atoms. For example, an Fe vacancy in the A sublattice surrounded by 6 NN Al atoms can be considered also as an Fe(A) vacancy in the $D0_3$ phase with two Al antisite atoms. Lifetimes of positrons trapped in Fe vacancies in the $D0_3$ phase with various number of Al antisite atoms are shown in figure 2 as well. Clearly, these lifetimes differ only very slightly from those calculated for Fe vacancies in B2 phase surrounded by the same number of NN Al atoms.

The bulk positron lifetime in the disordered A2 phase fluctuates due to the random distribution of Fe and Al atoms. However, similarly to the B2 phase these fluctuations are rather small. The dispersion (standard deviation) of bulk positron lifetimes obtained from a set of randomly generated A2 supercells is only 0.3 ps. The mean value of bulk positron lifetimes for the A2 phase is shown in table 1.

Two extreme cases can be considered for vacancies in the A2 phase: (i) a vacancy completely surrounded by Fe atoms (i.e. 8 NN Fe + 6 2NN Fe atoms), and (ii) a vacancy completely surrounded by Al atoms (i.e. 8 NN Al + 6 2NN Al atoms). Positron lifetimes for these two extremes are shown in table 1. The lifetime of positrons trapped in a vacancy in the A2 phase varies between these extremes, i.e. in the range from 181 to 199 ps.

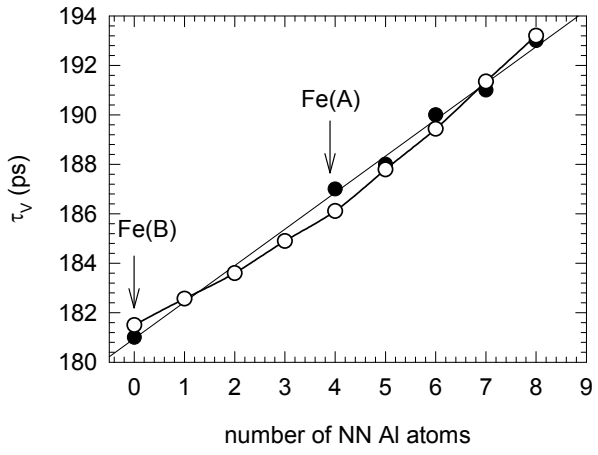

Figure 2. Calculated lifetimes of positrons trapped in Fe vacancies as a function of the number of NN Al atoms around vacancies. Open circles – B2 phase, Full circles $D0_3$ phase: Fe(A), Fe(B) vacancy and Fe(A) vacancy with various number of Al antisites.

4.2. LT and SPIS results

Both quenched alloys exhibit a single component LT spectrum with the corresponding positron lifetime τ_V shown in table 2. The lifetimes τ_V in both alloys are significantly longer than the Fe_3Al bulk positron lifetime τ_B = 112 ps [7] and fall into the range expected for vacancies. Hence, both alloys contain a high density of quenched-in vacancies, which causes saturated positron trapping. Comparison with theoretical calculations shows that experimental lifetimes τ_V are compatible with Fe vacancy in the B2 phase surrounded by 7 or 8 NN Al atoms, see table 1. Another possibility is that positrons are trapped in [001] Fe divacancies in the ordered $D0_3$ phase.

Table 2. Summarized experimental results for quenched $Fe_{75.99}Al_{24.01}$ and $Fe_{71.98}Al_{28.02}$ alloys: experimental lifetimes of positrons trapped at vacancies (τ_V), positron diffusion length measured by SPIS (L_+), concentration of quenched-in vacancies and (c_V) and microhardness (HV0.1).

sample	τ_V (ps)	L_+ (nm)	c_V (at.$^{-1}$)	HV0.1
$Fe_{75.99}Al_{24.01}$	190.8 ± 0.4	40 ± 6	$(4.8 \pm 0.6)\times10^{-4}$	412 ± 5
$Fe_{71.98}Al_{28.02}$	195.3 ± 0.5	4.0 ± 0.2	$(5.0 \pm 0.5)\times10^{-2}$	491 ± 5

The dependence of the S parameter on the energy of incident positrons measured by SPIS on quenched $Fe_{75.99}Al_{24.01}$ and $Fe_{71.98}Al_{28.02}$ alloys is plotted in figure 3. A local minimum of S at low energies 1-2 keV is due to positron annihilations in a thin oxide layer formed on the surface during annealing. One can see in figure 3 that the bulk value of the S parameter is higher in the $Fe_{71.98}Al_{28.02}$ alloy, i.e. in the alloy with higher Al content. The $S(E)$ curves were fitted by the VEPFIT software package [22] assuming two layers: (i) a thin oxide layer on surface, and (ii) the bulk alloy. In both alloys we obtained a good fit, which is plotted by solid lines in figure 3. Thickness of the oxide layer is around 10 nm and 30 nm in the $Fe_{71.98}Al_{28.02}$ and $Fe_{75.99}Al_{24.01}$ alloy, respectively. The positron diffusion lengths obtained from fits of the $S(E)$ curves in both alloys are shown in table 2. The $Fe_{71.98}Al_{28.02}$ alloy exhibits a shorter diffusion length than the $Fe_{75.99}Al_{24.01}$ alloy. This indicates that the $Fe_{71.98}Al_{28.02}$ alloy, i.e. the alloy with an enhanced Al content, contains more quenched-in vacancies compared to the other alloy.

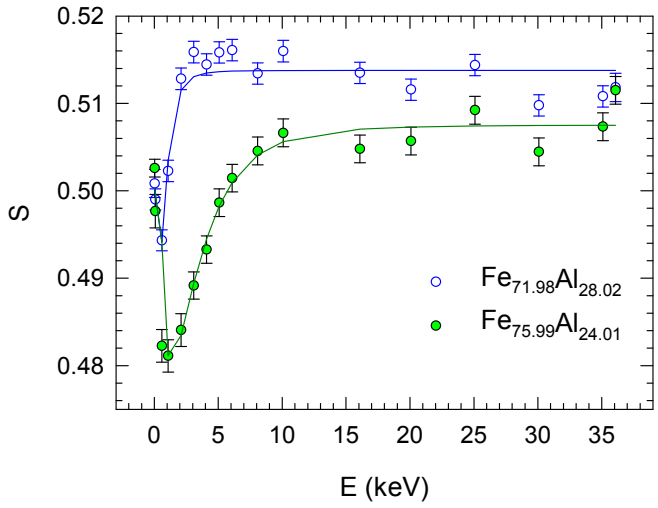

Figure 3. The dependence of the S parameter on the incident positron energy for $Fe_{75.99}Al_{24.01}$ and $Fe_{71.98}Al_{28.02}$ alloys measured by SPIS.

4.3. Estimation of concentration of quenched-in vacancies

The limit of vacancy concentration which causes saturated positron trapping can be estimated from the two-state trapping model. The positron trapping rate to vacancies can be calculated from the following equation

$$K = \frac{I_2}{I_1}\left(\frac{1}{\tau_B} - \frac{1}{\tau_V}\right) \qquad (2)$$

where τ_B = 112 ps is the positron bulk lifetime in Fe_3Al [7]. The free positron component cannot be resolved in an LT spectrum if its relative intensity I_1 falls below ≈ 5%. This corresponds to the positron trapping rate $K_{max,LT} \approx 7 \times 10^{10}$ at.s^{-1}. If the trapping rate $K \geq K_{max,LT}$, then saturated positron

trapping in vacancies takes place. The lowest concentration of vacancies which causes saturated positron trapping is

$$c_{V\,\max,\mathrm{LT}} = \frac{K_{\max,\mathrm{LT}}}{\nu_V} \approx 2.0\times10^{-4}\,\mathrm{at.}^{-1} \tag{3}$$

where we used the specific positron trapping rate $\nu_V = 4 \times 10^{14}$ at.s^{-1}, reported for vacancies in Fe_3Al in Ref. [7]. Clearly, the concentration of quenched-in vacancies in both alloys is higher than $c_{V\,\max,\mathrm{LT}}$.

The positron trapping rate K to vacancies can be also calculated from SPIS results

$$K = \frac{1}{\tau_B}\left(\frac{L_{+,B}^2}{L_+^2} - 1\right) \tag{4}$$

Here $L_{+,B}$ is the positron diffusion length in the defect-free material and L_+ is the positron diffusion length measured in the studied sample. The diffusion length $L_{+,B}$ is given by the equation

$$L_{+,B} = \sqrt{D_+\tau_B} \tag{5}$$

The positron diffusion coefficient D_+ in Fe_3Al was estimated as a weighted average of positron diffusion coefficients in Fe and Al

$$D_+ \approx \frac{3}{4}D_{+,Fe} + \frac{1}{4}D_{+,Al} = 3\ \mathrm{cm^2 s^{-1}} \tag{6}$$

The positron diffusion coefficients for pure Fe and Al were calculated using the deformation potential approximation [23].

The shortest positron diffusion length which can be determined by SPIS is $L_+ \approx 1$ nm. This corresponds to a limiting positron trapping rate $K_{\max,\mathrm{SPIS}} \approx 3 \times 10^{14}$ at.s^{-1}. Hence, using SPIS it is possible to determine even very high concentrations of vacancies. The upper limit of vacancy concentration measurable by SPIS is

$$c_{V\,\max,\mathrm{SPIS}} = \frac{K_{\max,\mathrm{SPIS}}}{\nu_V} \approx 0.7\ \mathrm{at}^{-1}\,. \tag{7}$$

Obviously the upper limit given by equation (7) is extremely high concentration, which cannot be reached in any real material. Thus, we can conclude that SPIS is able to determine even very high concentrations of vacancies and there is actually no upper limit of vacancy concentration measurable by this technique.

The concentration of quenched-in vacancies in the studied alloys determined from SPIS results is shown in table 2. Both studied alloys exhibit significant concentrations of vacancies, in particular $Fe_{71.98}Al_{28.02}$ contains extremely high concentration of vacancies, which is two orders of magnitude higher than in $Fe_{75.99}Al_{24.01}$. A higher concentration of vacancies in $Fe_{71.98}Al_{28.02}$ alloy is in concordance with higher hardness measured on this alloy. Hence, the concentration of vacancies and the hardness of the alloy increase with the increasing Al content. Coincidence Doppler broadening studies of quenched $Fe_{75.99}Al_{24.01}$ and $Fe_{71.98}Al_{28.02}$ alloy revealed that quenched-in vacancies are surrounded predominantly by Al atoms in the NN sites [24]. This finding is in agreement with lifetimes τ_v measured in these alloys, which are comparable with the lifetimes calculated for Fe vacancy surrounded by 7 or 8 NN Al atoms.

5. Conclusions

In the present work we studied $Fe_{75.99}Al_{24.01}$ and $Fe_{71.98}Al_{28.02}$ alloys quenched from 1000°C. Both alloys contain a high concentration of quenched-in Fe vacancies, which are surrounded predominantly

by nearest neighbor Al atoms. The concentration of quenched-in vacancies was determined from positron diffusion length measured by SPIS. The $Fe_{71.98}Al_{28.02}$ alloy exhibits significantly higher concentration of vacancies. Thus, the vacancy concentration increases with the increasing Al content. A higher concentration of vacancies in $Fe_{71.98}Al_{28.02}$ alloy is in concordance with higher hardness measured on this alloy. This testifies a strong influence of vacancies on mechanical properties of Fe_3Al based alloys.

Acknowledgement
We are grateful to M.J. Puska for his ATSUP code that served as a basis for further developments. This work was supported by the Czech Scientific Foundation (contract № GA106/08/P133) and by the Ministry of Education, Youths and Sports of the Czech Republic through the research plan № MSM 0021620834.

References

[1] Ho K and Dodd R A 1978 *Scr. Metall.* **12** 1055
[2] Liu T, Lee E H and McKammy C G 1989 *Scr. Metall.* **23** 875
[3] Jordan J L and Derbi S C 2003 *Intermetallics* **11** 507
[4] Sassi O, Aride J, Bernardini J and Moya G 1998 *Ann. Chim. Sci. Mat.* **23** 421
[5] Hautojärvi P 1979 *Positrons in Solids*, ed Hautojärvi P (Springer-Verlag, Berlin)
[6] Hautojärvi P and Corbel C 1995 *Positron Spectroscopy of Solids, Proceedings of The International School of Physics "Enrico Fermi"*, ed Dupasquier A and Mills A P (IOS Press, Amsterdam) p 491
[7] Schaefer H E, Würschum R, Šob M, Žák T, Yu W Z, Eckert W and Banhart F 1990 *Phys. Rev. B* **41** 11869
[8] Schaefer H E, Damson B, Weller M, Arzt E and George E P 1997 *Phys. Stat. Sol. (a)* **160** 531
[9] Jirásková Y, Schneeweiss O, Šob M, Novotný I, Procházka I, Bečvář F, Sedlák B, Šebesta F and Puska M J 1995 *J. Physique* **5** C1-157
[10] de Diego N, Plazaola F, Jiménez J A, Serna J and del Río J 2005 *Acta Mater.* **53** 163
[11] *Binary Alloy Phase Diagrams*, ed Massalski T B (Americal Society for Metals, Metals Park, Ohio, 1986)
[12] Puska M J and Nieminen R M 1983 *J. Phys. F* **13** 333; Seitsonen A P, Puska M J and Nieminen R M 1995 *Phys. Rev. B* **51** 14057
[13] Wakiyama T 1972 *J. Phys. Soc. Jpn.* **32** 1222
[14] Boroński E and Nieminen R M 1986 *Phys. Rev. B* **34** 3820
[15] Barbiellini B, Puska M J, Torsti T and Nieminen R M 1995 *Phys. Rev. B* **51** 7341
[16] Bečvář F, Čížek J, Procházka I and Janotová J 2005 *Nucl. Instr. Meth. A* **539** 372
[17] Bečvář F, Čížek J and Procházka I 2008 *Acta Physica Polonica A* **113** 1279
[18] Bečvář F 2007 *Nucl. Instr. Meth. B* **261** 871
[19] Anwand W, Kissener H R and Brauer G 1995 *Acta Physica Polonica A* **88** 7
[20] Barbiellini B, Puska M J, Korhonen T, Harju A, Torsti T and Nieminen R M 1996 *Phys. Rev. B* **53** 16201
[21] Campillo Robles J M, Odo E and Plazaola F 2007 *J. Phys.: Condens. Matter* **19** 176222
[22] van Veen A, Schut H, Clement M, de Nijs J, Kruseman A and Ijpma M 1995 *Appl. Surf. Sci.* **85** 216
[23] Bardeen J and Shockley W 1950 *Phys. Rev.* **80** 72
[24] Melikhova O, Čížek J, Kuriplach J, Procházka I, Cieslar M, Anwand W and Brauer G 2010 *Intermetallics* **18** 592